Bioelectrochemistry 133 (2020) 107462

Contents lists available at ScienceDirect

Bioelectrochemistry

journal homepage: www.elsevier.com/locate/bioelechem

Dual atom transfer radical polymerization for ultrasensitive electrochemical DNA detection

Xiaoke Zheng [a], Qianrui Liu [b], Manman Li [a], Weisheng Feng [a,*], Huaixia Yang [a], Jinming Kong [b,*]

[a] Pharmacy College, Henan University of Chinese Medicine, Zhengzhou 450046, PR China
[b] School of Environmental and Biological Engineering, Nanjing University of Science and Technology, Nanjing 210094, PR China

ARTICLE INFO

Article history:
Received 17 August 2019
Received in revised form 16 January 2020
Accepted 16 January 2020
Available online 28 January 2020

Keywords:
Electrochemistry
Biosensor
Dual surface-initiated polymerization
DNA

ABSTRACT

Atom transfer radical polymerization as a form of controlled/living radical polymerization is particularly attractive. In this work, dual atom transfer radical polymerization (ATRP) is reported for ultrasensitive DNA detection. Firstly, a peptide nucleic acid (PNA) modified with a thiol group was self-assembled on an electrode surface to capture target DNA (TDNA). The initiator of the first ATRP (ATRP-1), α-bromoisobutyric acid (BIBA), was linked to forming PNA/DNA heteroduplexes via coordination of Zr^{4+}. The polymer chain formed by the monomer of ATRP-1 (2-(2-bromoisobutyryloxy) ethyl methacrylate, BIEM) was also one of initiators of the second ATRP (eATRP-2). The other initiator of eATRP-2 was additional BIBA. ATRP-1 involves activator regeneration by electron transfer (ARGET) ATRP, regulated via excess reducing agent. eATRP-2 is electrochemically mediated ATRP which can control the polymerization via an appropriate applied potential. Compared with one ATRP, more monomers of eATRP-2 modified with ferrocene are attached to electrode surface. Under optimal conditions, this dual ATRP strategy provides a low limit of detection (25 aM, ~150 molecules) with satisfactory selectivity and stability. Importantly, this strategy presents a useful prospect for the field of biomolecule detection.

1. Introduction

The term biomarker generally refers to measurable biomolecules for diagnosis and prognosis [1]. Real-time monitoring of biomarkers may be of great help for the early diagnosis of a range of diseases [2]. Nevertheless, disease-related nucleic acids are at extremely low levels in the early stages of a disease. Also, diagnostic devices need to be portable, highly sensitive and inexpensive in practical applications. A biosensor is usually applied to detect biomolecules quantitatively, and has powerful practicability due to its advantages of miniaturization, low cost and high sensitivity [3]. Therefore, it has always been a focus in the field of analytical chemistry. For the above reasons, it is also of great significance to improve the sensitivity of biosensor for biomolecules detection.

Over the years, many strategies have been proposed to improve the sensitivity of a biosensor. The ways for improving the detection signal commonly use catalytic labels, nanoparticles and polymeric electroactive probes [4–6]. Amongst those strategies, the introduction of polymeric electroactive probes is a direct way to achieve signal amplification. Radical polymerization is one of widespread ways of forming polymeric materials. Macromolecules with uniform size and predetermined molecular weight are synthesized via surface-initiated controlled/living radical polymerization (SI-CRP) [7–9]. Amongst those radical polymerization techniques, atom transfer radical polymerization (ATRP) is widely applied for surface modification by virtue of its precisely controlled molecular weight and unprecedented control over polymerization [10,11]. More importantly, the length of polymeric chains is uniform because of the relatively low disparities (M_w/M_n < 1.1) of ATRP [12]. It is worth noting that many efforts have been made to reduce the usage of metal catalyst, and the essential issue is the regeneration of activator (metal complex with lower oxidation state) from deactivator which is metal complex with higher oxidation state. Activator regeneration by electron transfer (ARGET) ATRP is that deactivator continuously accumulated in the reaction system is reduced to activator by using excess reducing agent [13–15]. Furthermore, many ways can be utilized to regulate ATRP, and electrochemically mediated ATRP (eATRP) is particularly outstanding from those methods [16–20]. An applied potential is provided via electrochemical technologies to start ATRP, and high valence metal cation is reduced to low valence metal cation *in-situ* [21]. Thus, the amount of metal catalyst in this system can be well controlled via applied potential to reduce the use of metal catalysts. More importantly, eATRP can also improve the oxygen tolerance during an eATRP process [22]. Recently, eATRP has developed rapidly in

* Corresponding authors.
E-mail addresses: fwsh@hactcm.edu.cn (W. Feng), j.kong@njust.edu.cn (J. Kong).

https://doi.org/10.1016/j.bioelechem.2020.107462
1567-5394/

surface modification [23,24], and ATRP reacted in aqueous solvent has greatly promoted the functionalization of biomolecules [25]. Therefore, eATRP can be utilized to achieve ultrasensitive detection of biological molecules via introducing a large number of electroactive probes. Bontempo et al. reported a protein-polymer conjugate complex via streptavidin as the initiator of ATRP [26]. Yuan and coworkers have proposed an immunosensor to achieve ultrasensitive detection of TNF-α based on surface-initiated ATRP [27].

Inspired by the above opinion, we demonstrated a novel strategy to achieve highly sensitive DNA detection by dual ATRP in this work. A thiolated peptide nucleic acid (PNA) is modified onto an electrode surface by Au-S to capture TDNA. The first ATRP (ATRP-1) is (ARGET) ATRP, and the initiator of ATRP-1(α-bromoisobutyric acid, BIBA) is introduced to the electrode surface by phosphate-Zr^{4+}-carboxylate chemistry. The external stimuli of ATRP-1 is reducing agent, and high valence metal catalyst is reduced to low valence metal catalyst *via* ascorbic acid. More importantly, the polymeric chains formed by ATRP-1 monomer (pBIEM) are also one of initiators of the second ATRP (eATRP-2). The polymeric chains (pBIEM) and extra BIBA are both used as eATRP-2 initiators. eATRP-2 is activated via electrochemical techniques. Compared with one ATRP [1], more monomers modified with electroactive probes are attached to the electrode surface. The sensitivity of electrochemical DNA biosensor has been extremely improved, and the selectivity and practicality in human serum is satisfactory. Moreover, it has relatively clinical applicability due to the advantages of low cost and portable.

2. Experimental section

2.1. Materials and reagents

The details was seen in the Supplementary Material.

2.2. Apparatus

The details was seen in the Supplementary Material.

2.3. Preparation of this DNA electrochemical biosensor

The pretreatment of Au electrode was according to our previous work [28]. PNA (0.5 μM, 5.0 μL) was dropped onto an Au electrode surface, and the electrode was kept at 37 °C for 1.5 h, following by rinsing with ultrapure water. The PNA-modified electrode was immersed into 2.0 mM MCH which was dissolved in 70% ethanol at 37 °C for 0.5 h to block the nonspecific binding sites. After washing with 70% ethanol and ultrapure water respectively, TDNA (10 μL) was added onto the electrode surface, and the electrode was incubated at 37 °C for 1.5 h to form PNA/DNA heteroduplexes. Subsequently, the modified electrode was washed with Tris-HCl buffer to remove the unhybridized TDNA. Afterwards, 5.0 mM $ZrOCl_2$ dissolved in 10% ethanol was used to incubate electrode at 37 °C for 15 min, following by washing with 10% ethanol and ultrapure water. Then the electrode was immersed into 1.0 mM BIBA at 37 °C for 0.5 h to attach the ATRP-1 initiator to the PNA/DNA heteroduplexes. Hereafter, 15% ethanol and ultrapure water were used to remove the unbound initiator. The electrode was immersed into 400 μL of ATRP-1 cocktail at 37 °C which contained 20 mM AA, 10 mM BIEM and 10 mM Cu(II)Br/Me_6TREN to introduce the ATRP-1 monomer (BIEM). The electrode was washed with DMF and ultrapure water. Then, the electrode was immersed into the eATRP-2 cocktail which contained 8.0 mL of 0.1 M KPF_6, 0.1 mL of 10 mM Cu(II)Br/Me_6TREN, 0.1 mL of 10 mM FMMA and 1.8 mL DMF, and the electroactive probe (FMMA) was attached to the electrode surface via eATRP-2. eATRP-2 is stimulated under a potentiostatic condition. Immediately, LSV (Potential range: 0 V to 0.2 V; Scan rate: 1.0 V s^{-1}) was applied to treat electrode, then DMF and ultrapure water were used to rinse electrode surface to remove residual Cu(0) and FMMA. Finally, 1.0 M $LiClO_4$ as supporting electrolyte was employed to monitor the oxidation current of FMMA via SWV and the potential range was 0 V–0.6 V [29]. The construction process of this DNA electrochemical biosensor was illustrated in Schematic 1.

3. Results and discussion

3.1. The principle of this biosensor

In this work, PNA was employed as immobilized probe to capture TDNA. The affinity of PNA/DNA heteroduplexes is higher than DNA/DNA double helix due to weaker electrostatic repulsion in PNA/DNA heteroduplexes than that in DNA/DNA double helix. It was note that PNA was without phosphate groups which guaranteed that Zr^{4+} was only attached to TDNA. Subsequently, the initiator of ATRP-1 was introduced to the electrode surface *via* phosphate-Zr^{4+}-carboxylate chemistry, then dual ATRP began.

The mechanism of dual ATRP was illustrated in Schematic 2. ATRP-1 was (ARGET) ATRP which was chemical stimuli to modulate ATRP. In the initiation of (ARGET) ATRP, deactivators (Cu(II)Br/Me_6TREN) were reduced to Cu(I)/Me_6TREN by excess reducing agent (AA) to activate polymerization, meanwhile, AA was oxidized to dehydroascorbic acid (DHA) [30,31]. In the chain extension of (ARGET) ATRP, activators (Cu(I)/Me_6TREN) snatched the halogen atom of dormant alkyl halides initiators (BIBA, R-Br)[13]. Then, initiating radicals (R**.**) were produced via this reaction, and Cu(I)/Me_6TREN was once more oxidized to Cu(II)Br/Me_6TREN [32]. The produced Cu(II)Br/Me_6TREN was reduced by AA to regenerate Cu(I)/Me_6TREN. Thus, Cu(I)/Me_6TREN activators were continuously regenerated *via* excess AA, and excess reducing agent also improved the oxygen tolerance of ATRP-1. ATRP-1 monomers (BIEM) were introduced to the electrode surface via R**.** propagating with BIEM and terminating to form polymer (pBEIM, R_n-Br), and pBEIM (R_n-Br) also acted as one of initiators of eATRP-2.

eATRP-2 was based on electrochemistry to regulate ATRP process. In the initiation of eATRP, Cu(II)Br/Me_6TREN were electrochemically reduced to Cu(I)/Me_6TREN *in situ* via accepting an electron to start polymerization under a negative potentiostatic condition [33,34]. In this process, electron was employed as 'reducing agents' which could prevent the byproducts during the regeneration of activator. In the chain extension of eATRP, the halogen atom of dormant species were seized by Cu(I)/Me_6TREN, and then Cu(II)Br/Me_6TREN was produced and returned back to eATRP cocktail, then Cu(I)/Me_6TREN regenerated by electrochemical method [1]. P_n**.** reacted with FMMA, and numerous electroactive probes were introduced to electrode surface [28]. It was worth noting that dormant species in eATRP-2 included R_n-Br forming in ATRP-1 and extra dormant alkyl halides initiators (BIBA, R-Br). A dynamic equilibrium was established between dormant species (R_n-Br or R-Br) and propagating radicals (P_n**.**) [29]. The above reactions were repeated, and long polymeric chains formed. Propagating radicals (Pn**.**) reacted with monomers (FMMA) and terminated to form polymeric chains.

3.2. The characterizations of this electrochemical DNA biosensor

Selection of an appropriate applied potential (E_{app}) is primary to activate eATRP-2 for reducing Cu(II)Br/Me_6TREN to Cu(I)/Me_6TREN. CV was employed to acquire E_{app} in eATRP cocktail before eATRP-2. In Fig. 1A, two pairs of redox peaks were shown which might respectively represent the redox of Cu(II) and FMMA. The potential

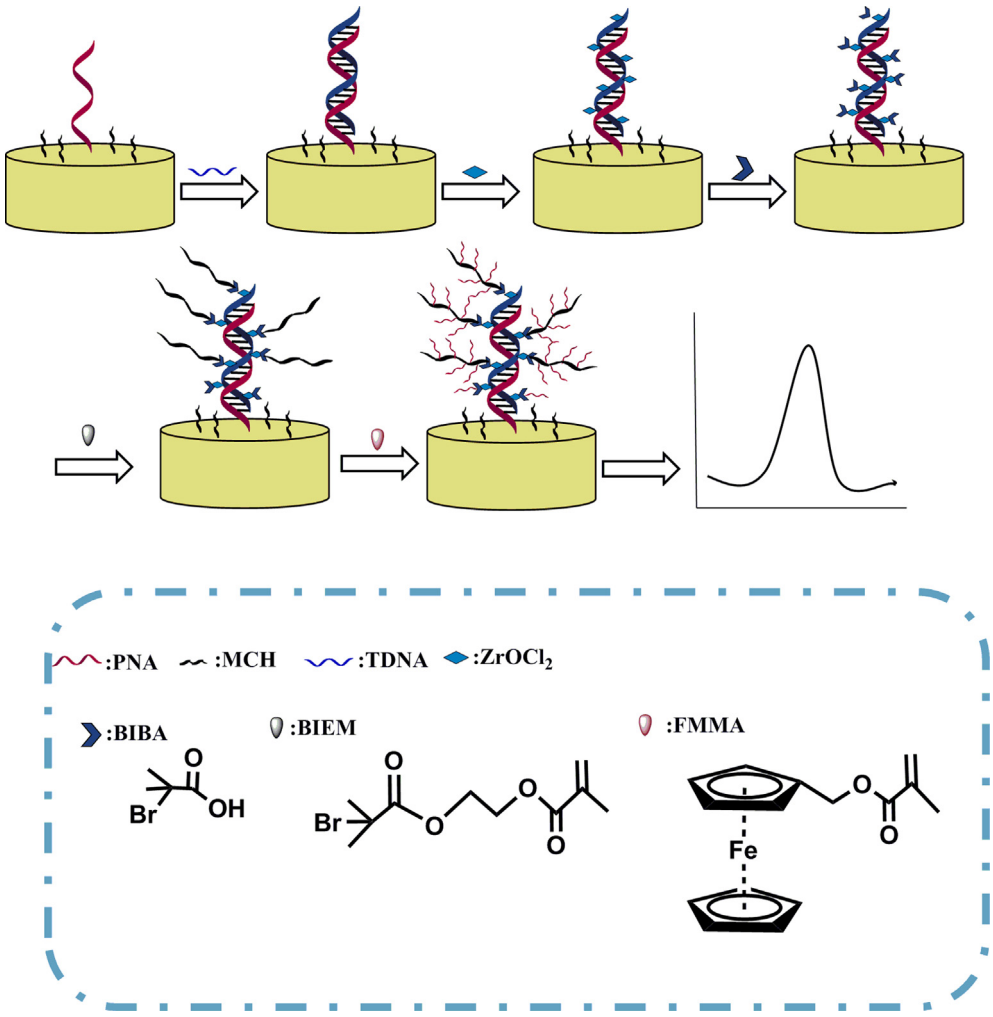

Schematic 1. The illustration of construction process of this DNA electrochemical biosensor.

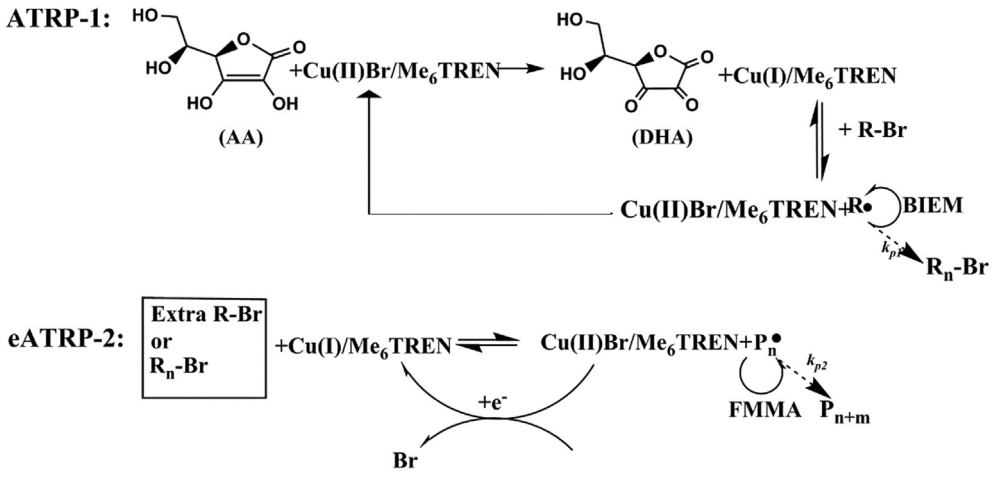

Schematic 2. The illustration of mechanism of this dual ATRP.

(−0.52 V) was chosen as the E_{app}, which could be seen from Fig. 1A. The cathode peak potential (−0.52 V) was the reduction potential of Cu(II) to Cu(I). At a more negative E_{app}, more Cu(II)Br/Me_6TREN could be reduced to Cu(I)/Me_6TREN at the electrode surface, according to Eq. (1):

$$E_{app} = E^{o} + \frac{RT}{F} \ln \frac{Cu(II)}{Cu(I)} \quad (1)$$

where E^o represents the standard potential (or half-wave potential) of the Cu(II)/Cu(I) couple [1], R and F is respectively gas constant

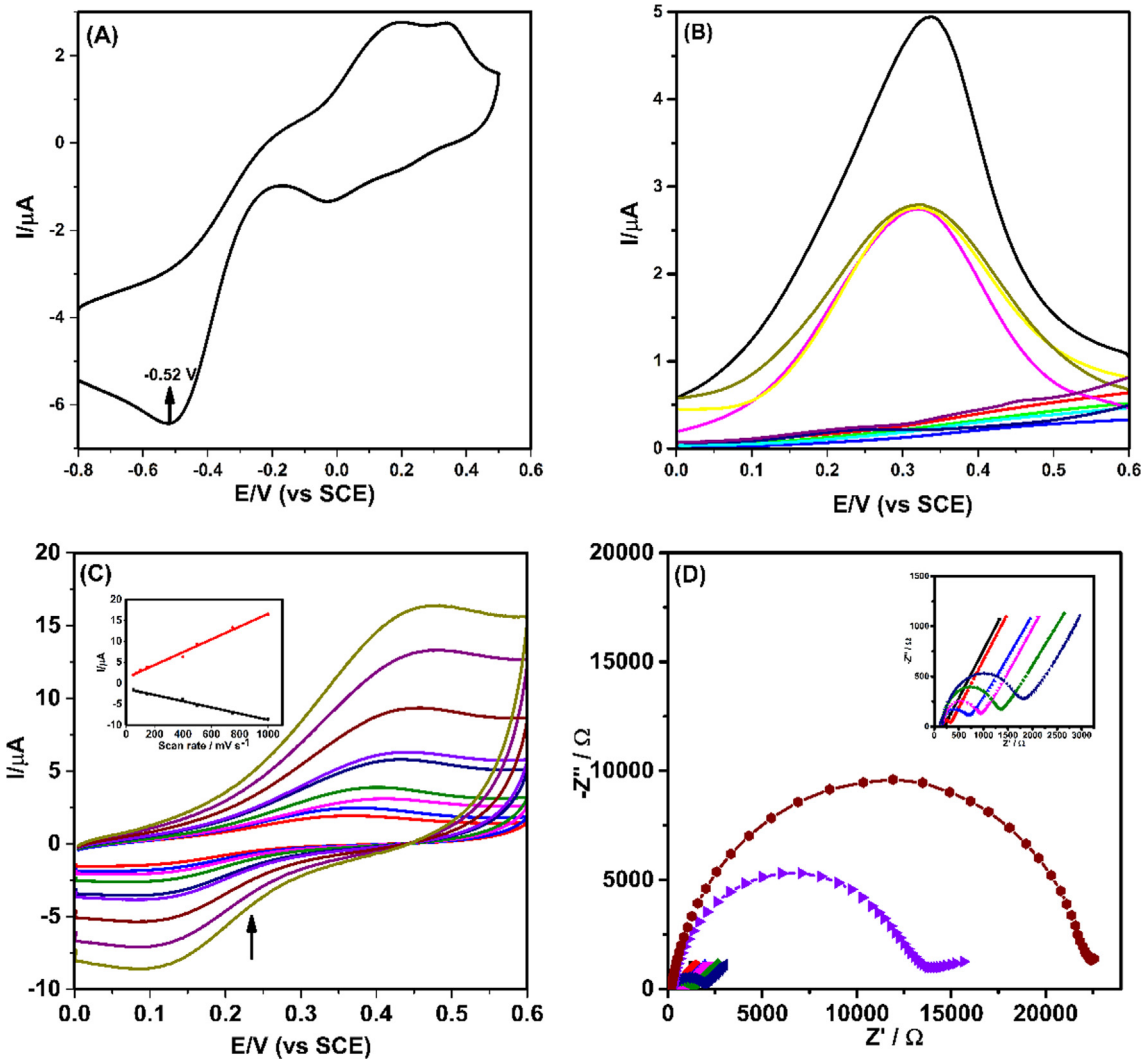

Fig. 1. (A) CVs of the PNA/MCH/TDNA/Zr^{4+}/BIBA/BIEM-modified Au electrode. Supporting electrolyte was eATRP cocktail. (B) SWVs of the PNA/MCH/TDNA/Zr^{4+}/BIBA/BIEM/FMMA-modified electrode (a, black line), and in the absence of PNA (b, red line), TDNA (c, green line), Zr^{4+} (d, blue line), BIBA (e, cyan line), BIEM (f, magenta line), Cu(II)Br/Me_6TREN-1 (g, yellow line), AA (h, dark yellow line), Cu(II)Br/Me_6TREN-2 (I, navy line) or FMMA (j, purple line). (C) CVs of the PNA/MCH/TDNA/Zr^{4+}/BIBA/BIEM/FMMA-modified electrode at different scan rates from 50 mV s^{-1} to 1000 mV s^{-1}. Inset: The linear relationship between anodic (red line) and cathodic (black line) peaks and scan rates. (D) The Nyquist plots of the bare gold electrode (a, black line), PNA (b, red line), PNA/MCH (c, blue line), PNA/MCH/TDNA (d, magenta line), PNA/MCH/TDNA/Zr^{4+} (e, olive line), PNA/MCH/TDNA/Zr^{4+}/BIBA (f, navy line), PNA/MCH/TDNA/Zr^{4+}/BIBA/BIEM (g, violet line) or PNA/MCH/TDNA/Zr^{4+}/BIBA/BIEM/FMMA-modified gold electrode (h, wine line).

and Faraday constant. However, polymerization rate would be too quick which resulted in out of control of polymerization. While E_{app} was more positive, the ratio of Cu(II)/Cu(I) would increase, and the control of polymerization was easier but polymerization rate would slow down. In view of above reasons, −0.52 V was selected as E_{app}.

SWV was applied to confirm the feasibility of ultrasensitive electrochemical detection of DNA via dual ATRP. The potential was from 0 V to 0.6 V, and the supporting electrolyte was 1.0 M $LiClO_4$. As shown in Fig. 1B, an obvious oxidation peak was observed at potential of 0.34 V, if all the reagents were present. The potential (0.34 V) was in the oxidation potential range of ferrocene into ferrocenium (Fig. 1B, a). Merely weak oxidation current could be seen in the absence of PNA (Fig. 1B, b). If PNA was not added into this biosensor, TDNA was not captured to electrode surface. Therefore, ATRP-1 initiator (BIBA) was not introduced to electrode surface by phosphate-Zr^{4+}-carboxylate chemistry. The disabled capture of ATRP-1 initiators led to the failure introduce of ATRP-1 monomer which also resulted in the failure introduce of eATRP-2 initiators. Likewise, if any of TDNA (Fig. 1B, c), Zr^{4+} (Fig. 1B, d) or BIBA (Fig. 1B, e) was absent from this biosensor, only weak oxidation current could be observed. If any of BIEM (Fig. 1B, f), Cu(II)Br/Me_6TREN-1 which is the catalyst of ATRP-1 (Fig. 1B, g) or AA (Fig. 1B, h) was not added, no oxidation peaks were observed. The absence of monomer, catalyst or reducing reagent of ATRP-1 led to the failure of ATRP-1. BIBA could be also used as alkyl halides initiators of eATRP-2, and eATRP-2 successfully reacted. Therefore, eATRP-2 monomers modified with ferrocene were also introduced to electrode surface. More importantly, the oxidation peak of dual ATRP (Fig. 1B, a) was obviously higher than that of one ATRP (Fig. 1B, f, g, h). This result also indicated that the sensitivity of this strategy via dual ATRP was improved when it was compared with one ATRP. If any of Cu(II)Br/Me_6TREN-2 which is the catalyst of eATRP-2 (Fig. 1B, i) or FMMA (Fig. 1B, j) was not added to biosensor, the anodic peaks were also feeble, suggesting that the initiator, catalyst and monomer was prerequisite of eATRP-2. Thus, FMMA was not successfully introduced to electrode surface. Those results verified that this method of ultrasensitive electrochemical DNA detection via dual ATRP amplification was feasible.

CV was utilized to characterize modified ferrocene on the electrode surface in 1.0 M $LiClO_4$, and scan rates were 50 mV s^{-1}, 75 mV s^{-1}, 100 mV s^{-1}, 150 mV s^{-1}, 300 mV s^{-1}, 400 mV s^{-1}, 500 mV s^{-1}, 750 mV s^{-1} and 1000 mV s^{-1}. The potential was from 0 V to 0.6 V. As shown in Fig. 1C, the anodic and cathodic peaks which were generated due to the redox of ferrocene presented a good linear relationship with different scan rates, indicating that the redox of ferrocene was not diffusion dependent. Namely, ferrocene was modified onto the electrode surface via covalent bond, which also indicated the feasible of ATRP. Thus, this strategy for ultrasensitive electrochemical DNA detection via dual ATRP was reliable.

EIS was employed to characterize the construction process of this biosensor in 0.1 M KNO_3 contained 5.0 mM $[Fe(CN)_6]^{3-/4-}$ with a frequency range from 0.1 Hz to 100 kHz, and the open circuit potential was 0.18 V. The diameter of hemicycle at high frequency represents charge transfer resistance (R_{ct}) of $[Fe(CN)_6]^{3-/4-}$ between electrode surface and electrolyte in Nyquist plots. The diameter of bare electrode was smallest as a result of fast charge transfer between interface of solution and electrode (~150 Ω, Fig. 1D, a). The R_{ct} gradually increased if PNA and MCH were modified onto electrode due to the obstacle of self-assembled molecular layer of PNA and MCH (~325 Ω and ~690 Ω, Fig. 1D, b-c). After modifying of TDNA to the electrode surface, R_{ct} further increased because of the steric hindrance and negatively charged phosphate backbone (~980 Ω, Fig. 1D, d). When $ZrOCl_2$ and BIBA were modified onto electrode surface, R_{ct} continuously increased due to further increase of steric hindrance (~1350 Ω and ~1810 Ω, Fig. 1D, e-f). An obvious increase of R_{ct} was observed after ATRP-1 and eATRP-2, indicating that polymeric chains of BIEM and FMMA were smoothly grafted on the electrode (~13800 Ω and ~22470 Ω, Fig. 1D, g-h). The above results indicated that the construction process of this electrochemical DNA biosensor was smooth and effective.

The morphology of Au electrode surface was characterized via AFM. As shown in Fig. S1, the surface height of PNA/MCH/TDNA/Zr^{4+}/BIBA-modified Au electrode was 25.8 nm (Fig. S1, A). After ATRP-1, the surface height of PNA/MCH/DNA/Zr^{4+}/BIBA/BIEM-modified Au electrode was 34.0 nm (Fig. S1, B). After the FMMA was modified onto electrode surface via eATRP-2, the surface height was 40.6 nm (Fig. S1, C). The height of electrode surface further increased. Those results suggested that this strategy was effective and successful.

3.3. The PNA self-assembled monolayer on Au electrode surface

The PNA was used as the capture probes of TDNA, and it was necessary to calculate the electrochemical parameters of PNA self-assembled molecular on the electrode surface. The finally current signal was directly related to area of Au electrode, therefore the effective area of Au electrode (A_{eff}) was firstly estimated. CV was applied to evaluate the A_{eff} in 0.1 M KNO_3 containing 5.0 mM $[Fe(CN)_6]^{3-}$, according to Eq. (2):

$$I_p = 2.69 \times 10^5 n^{\frac{3}{2}} A_{eff} D_o^{\frac{1}{2}} \upsilon^{\frac{1}{2}} C_O \quad (2)$$

where I_p is anodic peak current of $[Fe(CN)_6]^{3-}$, n is the electrons transferred of $[Fe(CN)_6]^{3-}$, A_{eff} is the effective area of Au electrode, D_o represented the diffusion coefficient of 5.0 mM $[Fe(CN)_6]^{3-}$ in 0.1 M KNO_3, υ and C_o is respectively scan rate of CV and the redox species concentration. As shown in Fig. S2, the I_p was 6.39×10^{-5} A, and the electrons transferred (n) of $[Fe(CN)_6]^{3-}$ was 1. The diffusion coefficient of 5.0 mM $[Fe(CN)_6]^{3-}$ in 0.1 M KNO_3 (D_o) was 2.4×10^{-6} cm^2 s^{-1} based on the Randle-Sevcik equation [35]. The scan rate of CV (υ) and redox species concentration (C_o) were respectively 1.0 V s^{-1} and 5 mM. Thus, the A_{eff} was 0.031 cm^2.

The surface coverage of PNA self-assembled molecular on Au electrode surface was estimated via EIS according to Eq. (3):

$$\theta = 1 - \left(\frac{R_{ct}^{Au}}{R_{ct}^{SAM}} \right) \quad (3)$$

where θ is surface coverage of PNA self-assembled molecular, R_{ct}^{Au} and R_{ct}^{SAM} are respectively the charge transfer resistance of bare Au electrode and PNA-modified electrode. As shown in Fig. 1D, R_{ct}^{Au} and R_{ct}^{SAM} were 150 Ω and 325 Ω. The surface coverage of PNA SAM (θ) was 0.538.

3.4. Optimization of conditions

The catalyst is one of prerequisites for ATRP. The ligand that forms complex with catalyst is a factor related to catalyst. The ligand plays a role in stabilizing the metal catalyst and increasing the solubility of complex. pH is a significant condition for the formation of Cu(II)Br/Me_6TREN and Cu(I)/Me_6TREN. When ATRP cocktail is under acidic conditions, ligand (Me_6TREN) is easily protonated that is unfavorable to the stability of Cu(II)Br/Me_6TREN and Cu(I)/Me_6TREN. When ATRP cocktail is alkaline, Cu(II)OH/Me_6-TREN would be formed because OH^- is easier to coordinate with Cu (II) than Br^-. Hence, pH = 7.0 was the appropriate pH of ATRP-1 and eATRP-2 in this strategy.

The ATRP time is also a significant factor for polymerization. It is important to optimize conditions to realize the best results. The peak current of ferrocene gradually increased before 90 min, then reached equilibrium which was observed in Fig. 2A. Therefore, 100 min was selected as the optimal time of ATRP-1. As shown in

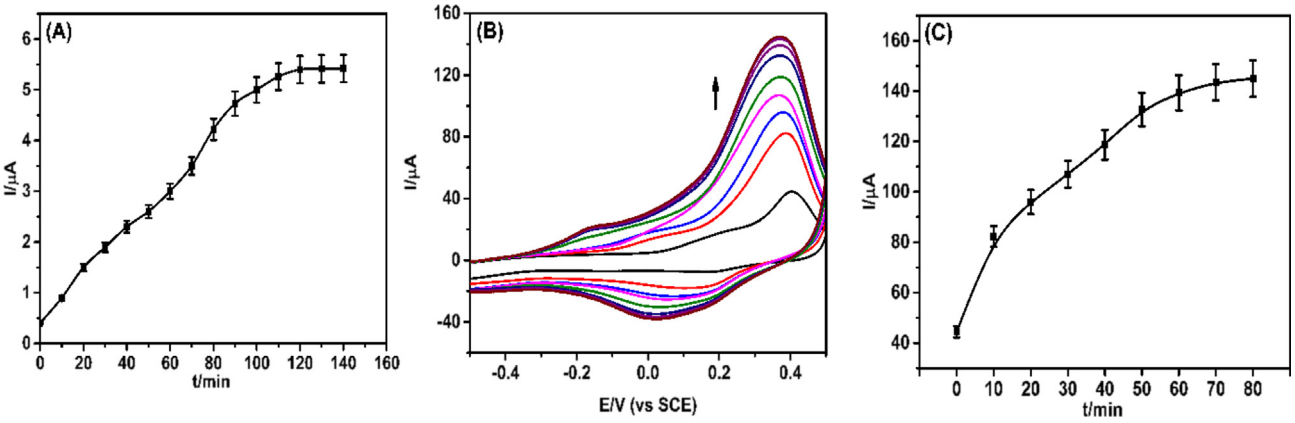

Fig. 2. (A) The effects of different ATRP-1 reaction time. (B) CVs of the PNA/MCH/TDNA/Zr^{4+}/BIBA/BIEM/FMMA-modified electrode in eATRP-2 cocktail. (C) The plots of oxidation peaks *versus* eATRP-2 time.

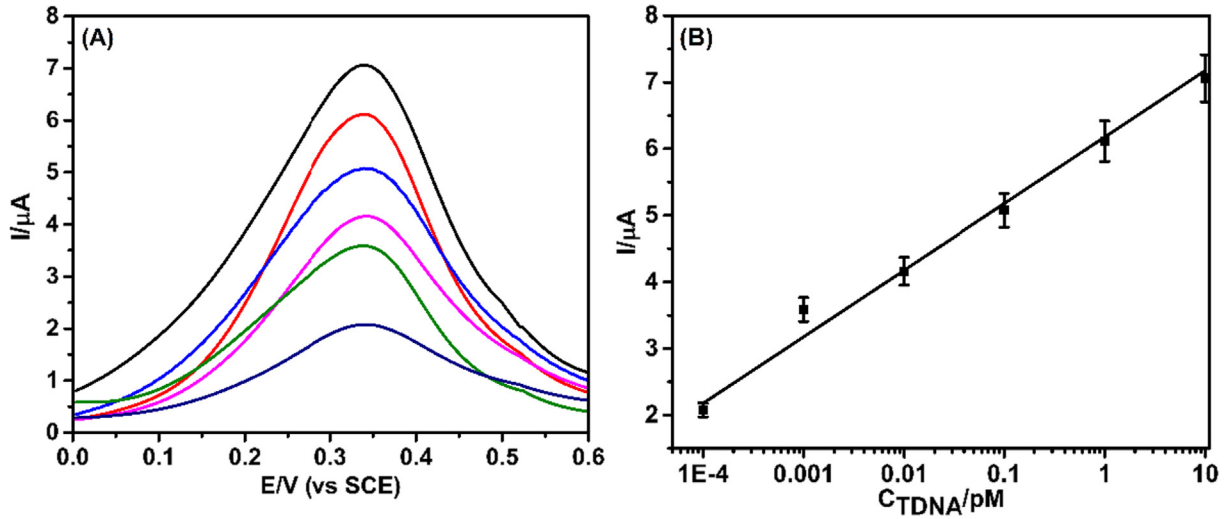

Fig. 3. (A) SWVs of different concentrations of 10 pM TDNA (a, black line), 1.0 pM TDNA (b, red line), 0.1 pM TDNA (c, blue line), 10 fM TDNA (d, magenta line), 1.0 fM TDNA (e, olive line), 0.1 fM TDNA (f, navy line). (B) The calibration plots between the oxidation current of ferrocene and the logarithm of TDNA concentration.

2C, CV was employed to real-time record oxidation current of ferrocene. At first 50 min the oxidation current increased, and then arrived at equilibrium. Thus, 60 min was chosen as appropriate time of eATRP-2.

3.5. Analytical performance

Under optimal conditions, SWV was utilized to detect different TDNA concentrations from 0.1 fM to 10 pM in 1.0 $LiClO_4$, and the potential was from 0 V to 0.6 V. An obvious peak was observed at the potential of 0.340 V from Fig. 3A, and peak current increased with the increase of TDNA concentrations. A good linear relationship was presented between peak current and the logarithm of different TDNA concentrations from 0.1 fM to 10 pM which was seen from Fig. 3B. The linear regression equation was I (μA) = 6.176 + 0.996 lg [C_{DNA}/pM] (R^2 = 0.98), and LOD was 25 aM (S/N = 3). As shown in Table 1, this LOD was much lower than many other methods. The numerous electroactive probes were modified onto the electrode surface *in situ* via dual ATRP. This strategy achieved ultrasensitive electrochemical DNA detection.

Table 1
Comparison of this method with other methods for DNA detection.

Method	Linear range	LOD	Refs
Colorimetry	0.02 pM-1 pM	0.01 pM	[36]
Electrochemistry	5 fM-80 pM	1.6 fM	[37]
Electrochemistry	100 fM-5 nM	92 fM	[38]
Electrochemistry	0.1 pM-100 nM	81 fM	[39]
Electrochemistry	0.1 fM-0.1 nM	72 aM	[1]
Electrochemistry	0.1 fM-10 pM	25 aM	This work

3.6. Selectivity analysis

The SWV responses of single base mismatched DNA (SBM), three bases mismatched DNA (TBM), and control DNA (CDNA) were compared with that from TDNA to access the selectivity of this strategy. As shown in Fig. 4, the SWV response of SBM is 26.2% of that from TDNA, revealing that this strategy for DNA detection presented satisfactory selectivity. The response of SBM is relatively high, which was because that a very small amount of DNA hybridized with PNA would lead to the attachment of ATRP

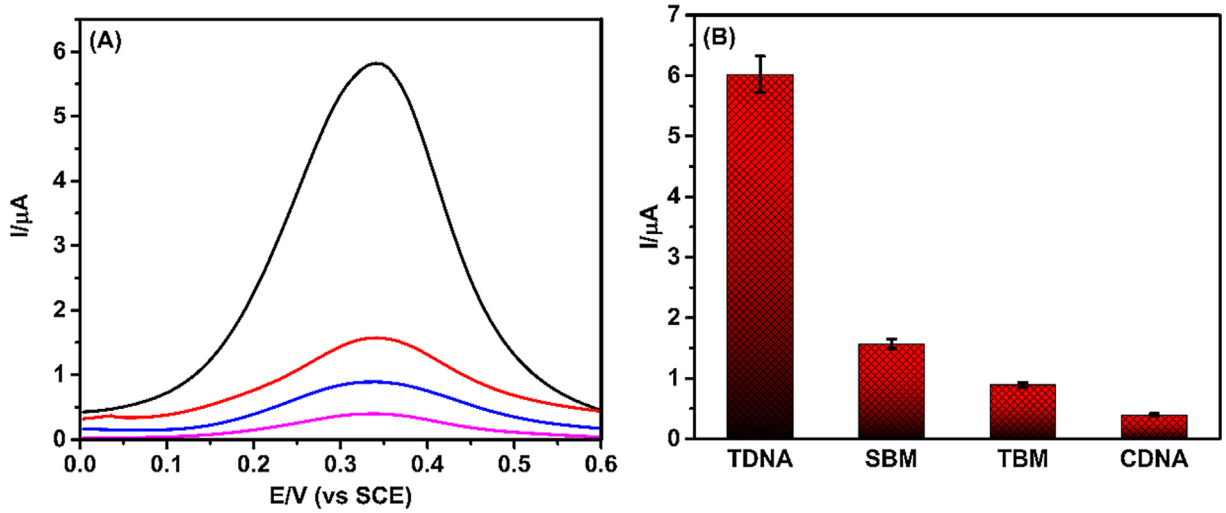

Fig. 4. (A) SWVs of TDNA (a, black line), SBM (b, red line), TBM (c, blue line) and CDNA (d, magenta line) in 1.0 $LiClO_4$. (B) SWV responses at the potential of 0.34 V toward TDNA, SBM, TBM and CDNA (1.0 pM, 10 μL).

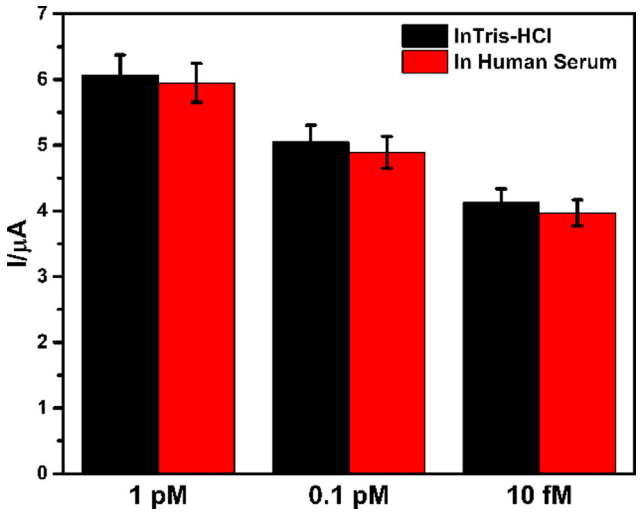

Fig. 5. SWV responses at the potential of 0.34 V toward 1 pM, 0.1 pM and 10 fM TDNA in Tris-HCl and human serum.

initiator via phosphate-Zr^{4+}-carboxylate chemistry and the high efficiency of dual ATRP caused the relatively high response of SBM. However, the SWV response of SBM (26.2%) was in acceptable range [1,4,29]. The SWV response of TBM is about 14.8% of that from DNA, and the SWV response of CDNA was almost same as background signal. While bases mismatched DNA hybridized with PNA, the number of phosphate groups was reduced due to high specificity of PNA/DNA heteroduplexes. Therefore, the amount of ATRP initiator introducing by phosphate-Zr^{4+}-carboxylate chemistry was greatly reduced, which led to a significant signal difference. Thus, this strategy showed a favorable selectivity.

3.7. Stability and reproducibility analysis

Biosensor is an instrument that is sensitive to biological substances, and it has the advantages of miniaturization, low cost and high sensitivity. The stability of the biosensor is one of important factor to evaluate this biosensor. The long-term stability of the electrode suggests that this biosensor has application value. To evaluate the stability of this dual amplified strategy, a long-term experiment was carried out. The prepared PNA/MCH/TDNA/Zr^{4+}/BIBA/BIEM/FMMA-modified electrode was stored in a moisture-saturated surrounding at 4 °C for 14 days. The SWV responses of those electrodes were compared with the response that came from the freshly prepared electrode, and the recovery was obtained. The recovery was 93.7%, suggesting that this strategy presented a satisfied stability.

The intra-assays and inter-assays were performed to assess the reproducibility of this biosensor for electrochemical DNA detection via dual ATRP. Seven repetitive assays were completed at TDNA concentrations of 10 pM, and the relative standard deviation (RSD) of intra- and inter-assays were respectively 4.27% and 4.51%. The above results suggested that this method had satisfied reproducibility.

3.8. Anti-interference of this strategy in human serum

To assess the anti-interference of this strategy, SWV was used to detect TDNA dissolved in human serum. 1 pM, 0.1 pM and 10 fM TDNA were dissolved in 5% human serum, and the SWV responses of TDNA from 5% human serum samples were respectively compared with that from 0.1 M Tris-HCl. As shown in Fig. 5, the SWV responses from 5% human serum were respectively 98%, 96.8%, 96.1% of that from the Tris-HCl for 1 pM, 0.1 pM and 10 fM TDNA. The anti-interference of this strategy was satisfactory, and presented certain potential in practical applications.

4. Conclusion

In summary, an ultrasensitive electrochemical DNA detection via dual ATRP amplification was firstly reported. The monomer of the first ATRP is also the initiator of the second ATRP. Thus, more monomers modified with electroactive probes of the second ATRP are attached to the electrode surface via dual ATRP. The sensitivity of electrochemical DNA biosensor is extremely improved, and the selectivity and practicality in human serum is satisfactory. Moreover, this strategy would be also applied to achieve various biomolecules detection.

Declaration of Competing Interest

The authors declared that there is no conflict of interest.

Acknowledgments

This work was supported by National Natural Science Foundation of China (21575066); the National Key Research and Development Project (The Major Project for Research of the Modernization of TCM): Key Technology Research for the Characteristic Chinese Medicine Industry Chain of Rehmannia glutinosa (2017YFC1702800); The Major Science and Technology Projects in Henan Province: Study on the key technology for quality control and the key characteristics of Rehmannia glutinosa, Dioscorea opposita Thunb and Achyranthes bidentata Blume from Henan Province (171100310500).

Appendix A. Supplementary material

Supplementary data to this article can be found online at https://doi.org/10.1016/j.bioelechem.2020.107462.

References

[1] Q. Hu, Q. Wang, G. Sun, J. Kong, X. Zhang, Electrochemically mediated surface-initiated de novo growth of polymers for amplified electrochemical detection of DNA, Anal. Chem. 89 (2017) 9253–9259.
[2] H. Sikes, R. Hansen, L. Johnson, R. Jenison, J. Birks, K. Rowlen, C. Bowman, Using polymeric materials to generate an amplified response to molecular recognition events, Nat. Mater. 7 (2008) 52–56.
[3] J. Wang, M. Leong, E. Leong, W. Sen Kuan, D. Leong, Clinically relevant detection of streptococcus pneumoniae with DNA-antibody nanostructures, Anal. Chem. 89 (2017) 6900–6906.
[4] Q. Hu, J. Kong, D. Han, L. Niu, X. Zhang, Electrochemical DNA biosensing via electrochemically controlled reversible addition-fragmentation chain transfer polymerization, ACS Sens. 4 (2019) 235–241.
[5] G. Liu, Y. Wan, V. Gau, J. Zhang, L. Wang, S. Song, C. Fan, An enzyme-based e-DNA sensor for sequence-specific detection of femtomolar DNA targets, J. Am. Chem. Soc. 130 (2008) 6820–6825.
[6] P. Ling, J. Lei, H. Ju, Porphyrinic metal-organic framework as electrochemical probe for DNA sensing via triple-helix molecular switch, Biosens. Bioelectron. 71 (2015) 373–379.
[7] A.J.D. Magenau, N. Bortolamei, E. Frick, S. Park, A. Gennaro, K. Matyjaszewski, Investigation of electrochemically mediated atom transfer radical polymerization, Macromolecules 46 (2013) 4346–4353.
[8] R. Barbey, L. Lavanant, D. Paripovic, N. Schuwer, C. Sugnaux, S. Tugulu, H. Klok, Polymer brushes via surface-initiated controlled radical polymerization: synthesis, characterization, properties, and applications, Chem. Rev. 109 (2009) 5437–5527.
[9] C.M. Hui, J. Pietrasik, M.R. Schmitt, C. Mahoney, J. Choi, M. Bockstaller, K. Matyjaszewski, Surface-Initiated polymerization as an enabling tool for multifunctional (nano-) engineered hybrid materials, Chem. Mater. 26 (2014) 745–762.
[10] J. Young, J. DeSimone, Frontiers in green chemistry utilizing carbon dioxide for polymer synthesis and applications, Pure Appl. Chem. 72 (2000) 1357–1363.

[11] E.H. Discekici, A. Anastasaki, J. Read de Alaniz, C.J. Hawker, Evolution and future directions of metal-free atom transfer radical polymerization, Macromolecules 51 (2018) 7421–7434.
[12] K. Matyjaszewski, Atom transfer radical polymerization (ATRP): current status and future perspectives, Macromolecules 45 (2012) 4015–4039.
[13] Y. Kwak, A.J.D. Magenau, K. Matyjaszewski, ARGET ATRP of methyl acrylate with inexpensive ligands and ppm concentrations of catalyst, Macromolecules 44 (2011) 811–819.
[14] A. Simakova, S. Averick, D. Konkolewicz, K. Matyjaszewski, Aqueous ARGET ATRP, Macromolecules 45 (2012) 6371–6379.
[15] W. Ma, H. Otsuka, A. Takahara, Poly (Methyl Methacrylate) grafted imogolite nanotubes prepared through surface-initiated ARGET ATRP, Chem. Commun. 47 (2011) 5813–5815.
[16] B. Li, B. Yu, W.T.S. Huck, W. Liu, F. Zhou, Electrochemically mediated atom transfer radical polymerization on nonconducting substrates: controlled brush growth through catalyst diffusion, J. Am. Chem. Soc. 135 (2013) 1708–1710.
[17] N. Bortolamei, A.A. Isse, A.J.D. Magenau, A. Gennaro, K. Matyjaszewski, Controlled aqueous atom transfer radical polymerization with electrochemical generation of the active catalyst, Angew. Chem. Int. Ed. Engl. 50 (2011) 11391–11394.
[18] Y. Wang, M. Fantin, K. Matyjaszewski, Electrochemically mediated atom transfer radical polymerization with dithiocarbamates as alkyl pseudohalides, J. Polym. Sci. A Polym. Chem. 57 (2019) 376–381.
[19] D. Li, X.Q. Niu, S.Y. Yang, Y.H. Chen, F. Ran, Thermo-responsive polysulfone membranes with good anti-fouling property modified by grafting random copolymers via surface-initiated eATRP, Sep. Purif. Technol. 206 (2018) 166–176.
[20] L.T. Strover, J. Malmström, L.A. Stubbing, M.A. Brimble, J. Travas-Sejdic, Electrochemically-controlled grafting of hydrophilic brushes from conducting polymer substrates, Electrochim. Acta. 188 (2016) 57–70.
[21] P. Chmielarz, P. Krys, S. Park, K. Matyjaszewski, PEO-b-PNIPAM copolymers via SARA ATRP and eATRP in aqueous media, Polymer 71 (2015) 143–147.
[22] S.S. Hosseiny, P. van Rijn, Surface initiated polymerizations via eATRP in pure water, Polymers 5 (2013) 1229–1240.
[23] P. Chmielarz, Synthesis of pyridoxine-based eagle-shaped asymmetric star polymers through seATRP, Polym. Adv. Technol. 12 (2017) 1787–1793.
[24] S. Park, P. Chmielarz, A. Gennaro, K. Matyjaszewski, Simplified electrochemically mediated atom transfer radical polymerization using a sacrificial anode, Angew Chem. Int. Ed. Engl. 54 (2015) 2388–2392.
[25] P. Chmielarz, Synthesis of α-d-glucose-based star polymers through simplified electrochemically mediated ATRP, Polymer 102 (2016) 192–198.
[26] D. Bontempo, H.D. Maynard, Streptavidin as a macroinitiator for polymerization: in situ protein−polymer conjugate formation, J. Am. Chem. Soc. 127 (2005) 6508–6509.
[27] L. Yuan, W. Wei, S. Liu, Label-free electrochemical immunosensors based on surface-initiated atom radical polymerization, Biosens. Bioelectron. 38 (2012) 79–85.
[28] Q. Liu, K. Ma, D. Wen, Q. Wang, H. Sun, Q. Liu, J. Kong, Electrochemically mediated atrp (eATRP) amplification for ultrasensitive detection of glucose, J. Electroanal. Chem. 823 (2018) 20–25.
[29] Q. Hu, Q. Wang, J. Kong, L. Li, X. Zhang, Electrochemically mediated in situ growth of electroactive polymers for highly sensitive detection of double-stranded DNA without sequence-preference, Biosens. Bioelectron. 101 (2018) 1–6.
[30] F. Stoffelbach, N. Griffete, C. Bui, B. Charleux, Use of a simple surface-active initiator in controlled/living free-radical miniemulsion polymerization under AGET and ARGET ATRP conditions, Chem. Commun. (2008) 4807–4809.
[31] K. Min, H. Gao, K. Matyjaszewski, Use of ascorbic acid as reducing agent for synthesis of well-defined polymers by ARGET ATRP, Macromolecules 40 (2007) 1789–1791.
[32] S.M. Paterson, D.H. Brown, T.V. Chirila, I. Keen, A.K. Whittaker, M.V. Baker, The synthesis of water-soluble PHEMA via ARGET ATRP in protic media, J. Polym. Sci. A Polym. Chem. 48 (2010) 4084–4092.
[33] P. Chmielarz, M. Fantin, S. Park, A.A. Isse, A. Gennaro, A.J.D. Magenau, A. Sobkowiak, K. Matyjaszewski, Electrochemically mediated atom transfer radical polymerization (eATRP), Prog. Polym. Sci. 69 (2017) 47–78.
[34] P. Chmielarz, S. Park, A. Sobkowiak, K. Matyjaszewski, Synthesis of beta-cyclodextrin-based star polymers via a simplified electrochemically mediated ATRP, Polymer 88 (2016) 36–42.
[35] C.A. Schroll, S. Chatterjee, W.R. Heineman, S.A. Bryan, Semi-infinite linear diffusion spectroelectrochemistry on an aqueous micro-drop, Anal. Chem. 83 (2011) 4214–4219.
[36] W. Yun, J. Jiang, D. Cai, P. Zhao, J. Liao, G. Sang, Ultrasensitive visual detection of DNA with tunable dynamic range by using unmodified gold nanoparticles and target catalyzed hairpin assembly amplification, Biosens. Bioelectron. 77 (2016) 421–427.
[37] Q. Wang, H. Zheng, X. Gao, Z. Lin, G. Chen, A label-free ultrasensitive electrochemical aptameric recognition system for protein assay based on hyperbranched rolling circle amplification, Chem. Commun. 49 (2013) 11418–11420.
[38] C. Tao, Y. Yan, H. Xiang, D. Zhu, W. Cheng, H. Ju, S. Ding, A new mode for highly sensitive and specific detection of DNA based on exonuclease III-assisted target recycling amplification and mismatched catalytic hairpin assembly, Chem. Commun. 51 (2015) 4220–4222.
[39] H. Wu, Y. Liu, H. Wang, J. Wu, F. Zhu, P. Zou, Label-free and ultrasensitive colorimetric detection of DNA based on target-triggered quadratic amplification strategy, Biosens. Bioelectron. 66 (2015) 277–282.